Regeneration of dust filters challenged with metallic nanoparticles: influence of atmospheric aging

KHIROUNI N.[1,2], CHARVET A.[2*], THOMAS D.[2], BEMER D.[1]

[1] Institut National de Recherche et de Sécurité (INRS), F-54519 Vandœuvre-lès-Nancy, France

[2] Université de Lorraine, CNRS, LRGP, F-54000 Nancy, France

*Corresponding author
E-mail: augustin.charvet@univ-lorraine.fr

Abstract
The aim of this study was to evaluate the regeneration efficiency of fibrous filters clogged with metallic ultrafine particles, as several complaints have been made by industrials in the metallurgical field about difficulties linked to the cleaning of filters. Aging of the dust deposits on the filters surface was also reported to be problematic. In this work, the metallic nanoparticles were generated by a pilot thermal spraying process using electric arc. Experiments were conducted on flat filters and the cleaning was performed using reverse pulse-jet. The regeneration efficiency was evaluated according to the residual pressure drop, the removed mass and the cleaned surface. Experiments revealed, under different conditions, a patchy inefficient cleaning of the clogged filters. The cleaning efficiency did not exceed 30% according to the removed mass. Clogging/unclogging cycles showed that the filtration process is highly instable as the residual pressure drop kept increasing very rapidly. The influence of atmospheric aging, i.e. exposure to different humidity conditions over time, on the filter cakes was investigated. Results showed that in presence of humidity a chemical reaction was responsible for making the deposit more adherent. The regeneration efficiency was reduced to 10% according to the removed mass after aging for 15 days under 80% humidity rate.

Keywords: Filtration, metallic nanoparticles, pulse-jet cleaning, regeneration efficiency

1. Introduction

Several industrial processes like thermal spraying, metal cutting and arc welding emit metallic nanoparticles. The efficient removal of these particles is of importance to ensure air quality in work places and to prevent their release into the environment due to their toxicity. Workers exposure to metallic fumes has been drawing a lot of attention recently (Falcone et al., 2018; Michalek et al., 2019; Bakri et al., 2019), especially since the classification of welding fumes as “Carcinogenic to humans” by the International Agency for Research on Cancer (Guha et al., 2017). It is estimated that millions of workers across the world are exposed to these fumes.

Metallurgical activities generate high concentrations of metallic ultrafine particles, the thermal spraying process being one of the most pollutant with concentrations that can reach 10^8 particles.cm^{-3} (Bémer et al., 2010). This process is widely used to apply protective coatings on different surfaces. Such activities are usually performed under ventilated booths and the fumes are directed towards dust collectors. Currently industrial filtration systems, namely fibrous media, are being challenged with a rapid increase of the pressure drop and an inefficient cleaning. The periodic cleaning of the filter elements is crucial to maintain an acceptable pressure drop across the filtration system and an acceptable airflow rate in the network. Failing to do so implies that a recurrent replacement of the filters is required, inducing by that higher operational costs. Indeed, the inefficient cleaning of filters exposed to thermal spraying fumes has been confirmed in the literature. Bémer et al. (2015) studied the cleaning efficiency of cartridge filters clogged with metallic ultrafine particles. The authors registered an inefficient cleaning using reverse pulse-jet, which led to a continuous and a rapid increase of the pressure drop. However, they did manage to clean the filter using a new cleaning system composed of a rotating probe with injection nozzles that is placed inside the filter cartridge and supplied with compressed air. Cho et al. (2020) also reported that the pulse-jet cleaning of a filter cartridge exposed to thermal spraying fumes is useless. Instead, the authors developed a new cleaning device, which consists of washing the loaded filter by injecting compressed air on the filter surface. Although these new cleaning methods could be associated with an important compressed air consumption, they might be suitable for small-scale dust collectors. Anyway, the available published data do show that metallic particles tend

to form a filter cake that is extremely adherent and difficult to detach.

Industrial feedbacks have also reported that aged deposits on the filters surface can sometimes be more problematic, as the filter cake undergoes some transformation that impedes its removal. First and Silverman (1963) noted that fine metallurgical dust deposits tend to have a high flow resistance and are extremely adherent. They stated that a common practice consists of an aging of the filter cake for some time in order to make its discharge easier. The authors attributed that to one of the three possibilities: agglomeration of the particles into larger ones, moisture adsorption or a discharge of the particles electrical charges. This implies that aging may indeed affect the cleaning efficiency, but no experimental data was provided. Nevertheless, exposure to humidity could have an effect on the filter cake behaviour. The influence of humidity is generally linked to the hygroscopicity of the particles. For hygroscopic particles, when the relative humidity exceeds the deliquescence point the aerosol particles exhibit a phase change which leads to a pressure drop increase that is characteristic of liquid aerosol (Joubert et al., 2010). Montgomery et al. (2015) studied the influence of exposing filter cakes to a higher humidity rate than that during loading. For deposits composed of hygroscopic particles (NaCl) and for humidity rates below the deliquescence point, a reduction of the pressure drop was observed. For non-hygroscopic particles (Al_2O_3) no variation was registered. The authors found that the effect of humidity on hygroscopic particles deposits was irreversible due to a structural change. Schmidt and Pilz (1996) reported that with increasing humidity during loading, the filter cake adhesion force tends to increase due to water adsorption. For limestone particles, the authors registered a decrease of the regeneration efficiency with increasing the relative humidity. It can be concluded that filter cakes exposed to moisture could face a modification of their structure leading to a variation of the deposit behaviour.

The aim of this work is to quantify the cleaning efficiency of flat filters clogged with metallic ultrafine particles using reverse pulse-jet, as there is not much available data about cleaning of fibrous media clogged with nanoparticles. The effect of atmospheric aging on the filter cake characteristics and adhesion is also of interest. Measurements of the filter cake resistance evolution during aging, under different humidity conditions, are performed in order to determine if a structural change takes place. The cleaning efficiency of aged deposits and the adhesion force are also evaluated.

2. Materials and methods

2.1. Experimental pilot

Particles are generated by a pilot thermal metal spraying process using electric arc that allows reproducing the real conditions encountered at an industrial scale. As shown by figure 1, the electric arc gun (M25 Margarido®) is fed by Zn/Al (85/15 %) wires and the melted metal is sprayed by compressed air on a rotating cylinder. The gun moves vertically in order to ensure applying a uniform layer over the cylinder surface. It should be mentioned that zinc and zinc alloys are the most used metallic elements for thermal spraying. The fumes generated are sucked through the main stainless steel pipe, of 20 cm diameter, towards the main filtration system with an air flow rate of 2000 $m^3.h^{-1}$. The entire pilot is grounded in order to avoid electrostatic losses during particles transport. The generated aerosol has been characterized in a previous work (Bémer et al., 2013). The fumes are composed of two particle populations: nanostructured particles formed from agglomeration of primary particles of 9 nm diameter and a micronic fraction (slag) with a median mass diameter of 9 µm measured with a DLPI (Dekati Low Pressure Impactor). The number distribution results, measured with an ELPI (Electrical low Pressure Impactor), showed that 90% of the particles are smaller than 100 nm. The average effective density was calculated from measurements obtained by coupling a Differential Mobility Analyser (DMA), an Aerosol Particle Mass Analyser (APM) and a Condensation Particle Counter (CPC) (Charvet et al., 2015). It was estimated to be around 0.6 $g.cm^{-3}$. The mean electric charge is smaller than 10^{-3} elementary charges/particle.

A sampling nozzle in the main canalisation allows directing a fraction of the fumes to the studied filtration system, which is composed of two filter holders, for conducting experiments on flat filters of 14 cm diameter. A cyclone (URG-2000-30EC®) with a cut diameter of 2.5 µm is placed ahead of the filter holders to eliminate coarse particles. An aerosol sampling was performed downstream of the cyclone. The number concentration is close to $2\ 10^8$ $particles.cm^{-3}$ with a mean mobility equivalent diameter of 70 nm. The particles size distribution, measured by a scanning mobility particle sizer (5.403 Grimm®) after dilution (VKL 100, Palas®), is given by figure 2. The air is sucked by a pump and sonic nozzles allow maintaining the face velocity at a constant value of 3 $cm.s^{-1}$. The pressure drop evolution during particles loading is measured by pressure sensors (Keller®). A cleaning system by reverse pulse-jet is integrated in the filter holders.

The cleaning is performed using an injection nozzle of 3 mm diameter, a pulse duration of 0.2 s and an air pressure of 4 bar. These conditions were chosen because they are commonly used for the cleaning of industrial filtration systems. The cleaning of the main filtration system is not investigated in this paper. Although the results acquired using flat filters are not the same as those with a full-scale industrial system, the aim is to obtain quantitative data on the influence of different operational parameters. Sampling on 47 and 25 mm diameter PVC filters (GLA 5000, Pall®) is also performed for characterising the deposits.

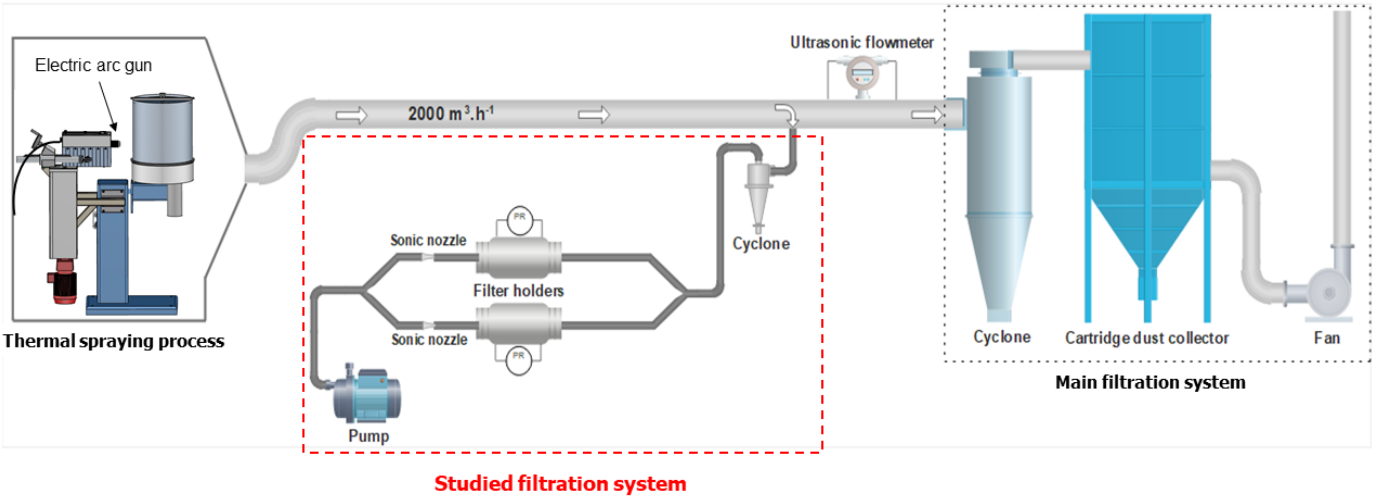

Figure 1: Experimental pilot

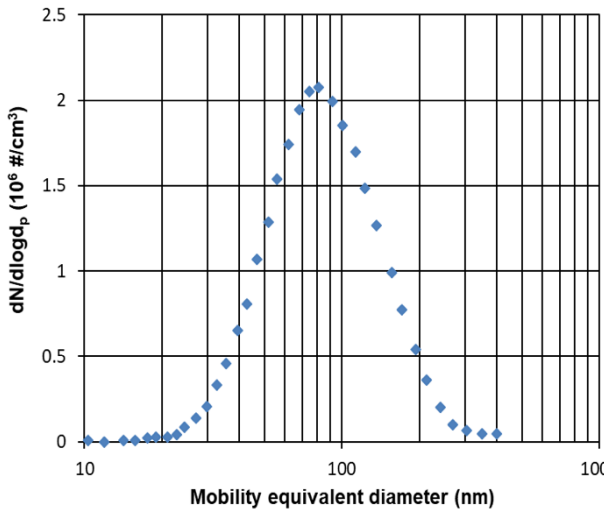

Figure 2: Number size distribution of the generated metallic particles after 1/100 dilution

The filter media used for the cleaning experiments is a corrugated cellulose fibre base medium with a nanofiber layer on its surface. Figure 3 gives a scanning electron microscope (SEM) image of the treated side. This type of medium is commonly used for the filtration of metallurgical dusts. Table 1 resumes the key characteristics of the filter.

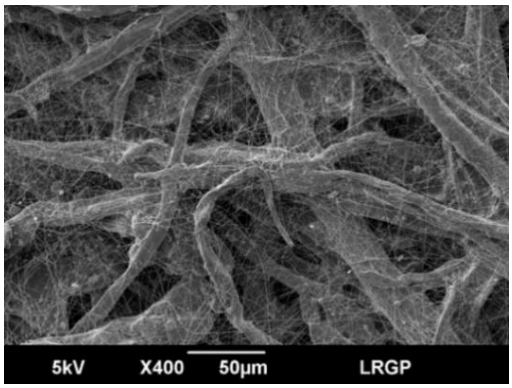

Figure 3: SEM image of the used filter medium

Table 1: Characteristics of the filter medium.

Composition	Cellulose
Surface treatment	Nanofibre layer
Average fibre diameter-Davies (µm)	23±1
Mean nanofibers dimeter (nm) [a]	212±74
Grammage (g.m^{-2})	138±2
Thickness (mm) [b]	0.28±0.02
Porosity [c]	0.70±0.06
Permeability (m^2)	3.62±0.18 10^{-11}

[a] Measurement by SEM image analysis; [b] Measurement by micrometer screw; [c] Measurement by pycnometry

2.2. Atmospheric aging of a metallic nanostructured filter cake

Filter cakes composed of metallic nanostructured particles with a weighed deposited mass of about 5±0.6 g.m^{-2}, sampled on 47 mm diameter PVC filters, were stored in dry and moist air conditions at a temperature of 15±2 °C. The use of these filters ensures avoiding depth filtration, which means that any registered changes will only be due to modifications of the cake structure. The clogged filters were kept inside their filter holders during all the storage duration in order to avoid any handling of the filter cakes. Humidity was controlled using the saturated salt solution method (Young, 1967). This method is based on the water vapour pressure equilibrium between the gas phase and the saturated solution in an enclosed chamber. The water vapour pressure is lower than that obtained with pure water due to the attraction of the water molecules by the salt ions in the solution. A saturated salt solution was placed in the bottom of a desiccator and sensors were used to monitor the humidity and the temperature during storage. The filter cakes were placed on a grid above the saturated salt solution. At the storage temperature, a NaCl saturated solution allows maintaining a relative humidity of 77% and a NaBr solution gives a relative humidity of 65%. Dry atmosphere is achieved by replacing the salt solution with a silica gel adsorbent. A filter cake was left to age under room conditions with a relative humidity of 30%. Permeation measurements were performed before and during storage to determine the effect of aging on the variation of the cake resistance, which was determined using the following expression:

$$\Delta P = R_f \mu U + R_c \mu U \quad (1)$$

Where ΔP is the measured pressure drop (after subtracting the filter holder pressure drop), U the air velocity, μ the air viscosity, R_f and R_C the filter and cake resistances respectively. Experiments performed on a clean PVC filter guaranteed that its resistance remained constant whatever the storage duration and conditions.

Aged deposits, sampled on 25 mm diameter filters, were characterized using X-Ray Diffraction (XRD) (Empyrea, Panalytical®) and Transmission Electron Microscopy (TEM) (JSM-2100 F, Jeol®). These filter cakes were left to age in dry and humid (70 % humidity) atmospheres at 15±5 °C for a 1-month period before analysis. A fresh deposit was also analysed for comparison.

2.3. Evaluation of the cleaning efficiency and adhesion force

The cleaning efficiency of flat filters (14 cm diameter) using reverse pulse-jet was evaluated according to three parameters: the residual pressure drop, the removed mass and the cleaned surface. The residual pressure drop and the removed mass measurements were performed in separate experiments, as weighing the filter cake before cleaning could disrupt the residual pressure drop value due to handling. The cleaned surface was evaluated by integrating a camera-endoscope in the filter holder that allows taking a picture after cleaning. Image analysis, performed using the software ImageJ®, is based on a binarization of images by a thresholding method. The greyscale images are then analysed to estimate the cleaned surface.

The regeneration efficiency according to the residual pressure drop is calculated as follows (Hau and Leung, 2016):

$$R_P = \frac{\Delta P_{Max} - \Delta P_r}{\Delta P_{Max} - \Delta P_i} \quad (2)$$

where ΔP_{Max} is the maximum value of the pressure drop before cleaning, ΔP_r the residual pressure drop after cleaning and ΔP_i the initial pressure drop of the clean filter.

The cleaning efficiency according to the removed mass is expressed as follows:

$$R_M = \frac{\text{Removed mass}}{\text{Initial cake mass}} \quad (3)$$

The cleaning efficiency according to the cleaned surface is determined by the following expression:

$$R_S = \frac{\text{Cleaned surface}}{\text{Total surface}} \quad (4)$$

In order to investigate the influence of atmospheric aging on the cleaning efficiency, filter cakes with a deposited mass of about 5±0.47 g.m^{-2} , formed using the studied filtration system given by figure 1 were stored in a climatic chamber (Excal, Climats®) under different humidity rates at a temperature of 15 °C for a duration of 15 days. The filter cakes were kept inside the filter holders during storage. After aging, the cleaning efficiency using reverse pulse-jet was evaluated.

The adhesion force between the filter cake and the filter medium was estimated using the reverse flow technic, which is commonly used in the literature and reported to give acceptable estimation (Seville et al., 1989; Silva et al., 1999; Tanabe et al., 2011; Li et al., 2019a; Xie et al., 2020). This method consists on measuring the pressured drop of an airflow in the reverse direction of filtration across the filter and the cake (figure 4). For small air velocities, the measured pressure drop consists of the contribution of the

cake and the filter. Once reaching a certain critical velocity a part of the cake will detach from the filter. At that critical moment, the measured pressure drop minus the filter pressure drop represents the necessary force that must be applied to overcome the adhesion force of the filter cake. This pressure drop is expressed as:

$$\Delta P_C = R_f \, \mu \, U_C + F_{adh} \qquad (5)$$

where ΔP_C is the cleaning pressure drop, R_f the filter resistance, μ the air viscosity, U_C the cleaning velocity and F_{adh} is the adhesion force per unit area.

By plotting the measured cleaning pressure drop as a function of the cleaning velocity (values that exceed the critical value), the interception of the regression line with the ordinate axis represents the adhesion force per surface area, as shown by figure 5. The cleaning was performed with an air velocity between 6 and 30 $cm.s^{-1}$ and experiments were conducted on filter cakes with a deposited mass of 5±0.47 $g.m^{-2}$. The used cake loading is enough for cake formation on the filter surface.

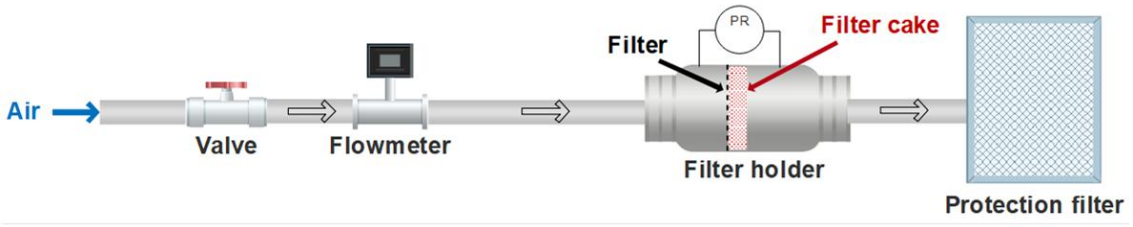

Figure 4: Experimental set up for measuring the adhesion force by the reverse flow method

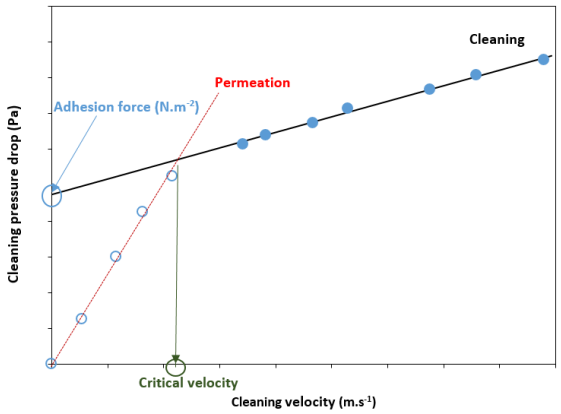

Figure 5: Measurement of the filter cake adhesion force using the reverse flow technic

3. Results and discussion

3.1. Effect of atmospheric aging on the filter cake

Figure 6 gives the evolution of the filter cake resistance during aging over a period of 22 days, presented as the ratio of the resistance after aging for a period of time (R_C) to the resistance of the fresh cake (R_{C0} = 6.7±0.84 10^9 m^{-1}). At an elevated humidity rate the cake resistance decreases considerably, whereas in a dry atmosphere or at a low humidity (RH= 30%) no significant variation is registered. The cake resistance seems to decrease more rapidly by raising the relative humidity from 65% to 77%. This variation of the cake resistance implies that the cake structure has been modified. Noting that the cake resistance is a function of the porosity, the deposited mass, the particles diameter and density. During the first hours of aging, and under all conditions, a decrease of the resistance is noted. This is more visible for the cake that aged under dry air. When the particle loading is stopped, the disassembly of the filter holder for storage might induce the creation of some cracks and consequently some preferential paths. This can explain the initial decrease of the pressure drop observed whatever the operational conditions. Following the first measurements, the cake structure tends to stabilize. After aging for 22 days under 77% relative humidity, the filter cake was dried by passing an air flux for several minutes. Afterwards, the cake resistance was measured and it remained the same, indicating that the transformation of the filter cake is not reversible. Measuring the evolution of the cake resistance is a simple way to determine whether the cake has undergone a transformation and its kinetics.

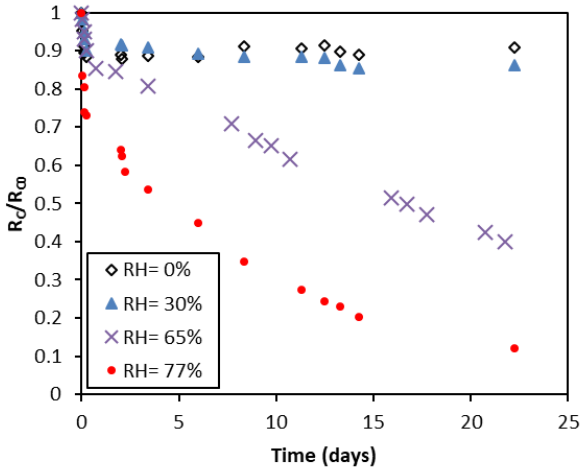

Figure 6: Evolution of the filter cake resistance during aging under different conditions at 15±2°C.

Nevertheless, it does not give us an insight on the nature of this modification, as it can be physical or chemical.

XRD analysis of aged deposits revealed that after storing in dry atmosphere there was presence of zinc oxide (ZnO), Zinc and Aluminium. The sample that aged in humid air (RH= 70%) showed the presence of an aditional component which is hydrozincite ($Zn_5(CO_3)_2(OH)_6$). Transmission Electron Microscopy (TEM) images of the aged deposits and a fresh one are given by figure 7. Between fresh and aged particles in dry air no differences are observed. Nevertheless, particles that were exposed to humidity exhibit the presence of a new crystalline phase.

This could help explain the decrease of the cake resistance. The TEM images of the aged particles under humidity clearly show a decrease of the particles specific area. Visual observations of the samples that aged under humidity showed that the cake colour turned form brown to white, which is characteristic of zinc hydroxyl-carbonate. Indeed, hydrozincite is a classic product of the atmospheric corrosion of zinc that is formed in the presence of water and CO_2. The formation of this product is favoured at high humidity, especially above 70% relative humidity.

The common reaction mechanism is given by equations 6 to 10 (Graedel, 1989; Falk et al., 1998; Almeida et al., 2000). At elevated humidity a water layer will be adsorbed on the metallic particles surface that will facilitate the formation of metal cations, zinc hydroxide and carbonate ions which will lead to the formation of hydrozincite (equation 10). It should be noted that the presence of other contaminants in the air, such as sulphur or chloride that might be present in industrial atmospheres, will lead to the formation of other products. Zinc oxide (ZnO) presence in the filter cake, as found by XRD results, is due to the oxidation of zinc during thermal spraying (arc temperature of about 6000 °C) and to exposure to atmospheric oxygen. Gankanda et al. (2016) studied the atmospheric aging of ZnO nanoparticles. They found that the reaction of atmospheric CO_2 and H_2O (at different relative humidity) with the nanoparticles was responsible for the formation of hydrozincite. The chemical reaction of the filter cake confirms the irreversibility of the transformation after exposure to high humidity.

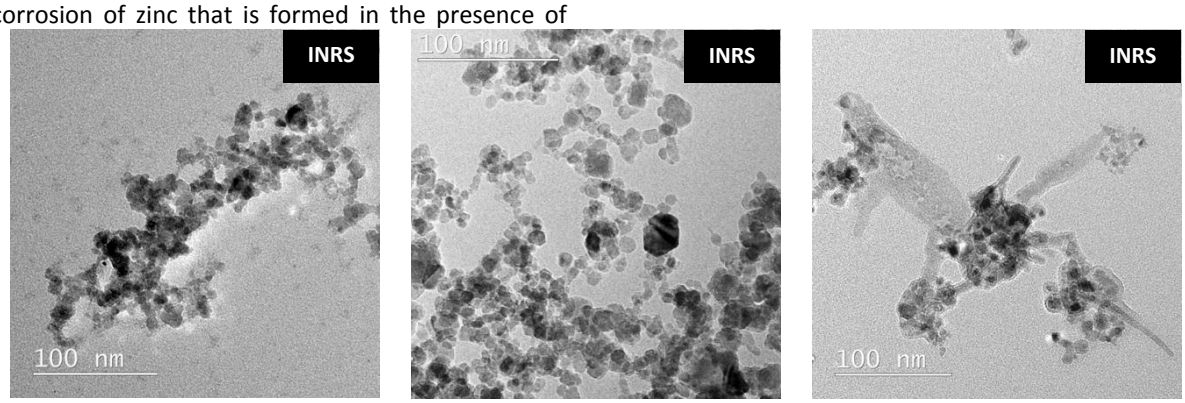

(a) **(b)** **(c)**

Figure 7: TEM images of fresh particles (a), aged particles in dry air (b) and aged particles under humidity (c).

$$Zn\ (s) \rightarrow Zn^{2+}\ (aq) + 2\ e^{-} \quad (6)$$

$$O_2\ (g) + 2\ H_2O\ (l) + 4\ e^{-} \rightarrow 4\ OH^{-}\ (aq) \quad (7)$$

$$H_2O\ (l) + CO_2\ (g) \rightleftarrows CO_3^{2-}\ (aq) + 2\ H^{+}\ (aq) \quad (8)$$

$$2\ Zn\ (s) + O_2\ (g) + 2\ H_2O\ (l) \rightarrow 2\ Zn(OH)_2\ (s) \quad (9)$$

$$Zn(OH)_2\ (s) + 4\ Zn^{2+}\ (aq) + 4\ OH^{-}\ (aq) + 2\ CO_3^{2-}\ (aq) \rightarrow Zn_5(CO_3)_2(OH)_6\ (s) \quad (10)$$

3.2. Cleaning efficiency results

Measurements of the cleaning efficiency using flat filters (of 14 cm diameter) as a function of the deposited mass and the number of cleaning pulses are given by figure 8. The maximum pressure drop value before cleaning is specified in the secondary abscissa axis. For only small collected masses, the pressure drop reaches significant values that exceed 2000 (Pa), which generally represents the maximum limit value for industrial filtration systems. A gap is registered between the cleaning efficiency according to the residual pressure drop and to the removed mass and cleaned surface. Visual observations confirm that we are dealing with a patchy inefficient

cleaning in the form of small holes across the surface. Therefore, once these holes are formed in the filter cake, the pressure drop decreases because the air will preferentially pass through them as they constitute low resistance zones. At best the removed mass and cleaned surface do not exceed 30% which indicates that most of the filter cake is still adhering to the filter surface. Hence, the residual pressure drop, which is the most used parameter at an industrial scale, may not provide an accurate evaluation of the cleaning efficiency in the case of adhesive ultrafine dusts. The removed mass and the cleaned surface give close estimation of the cleaning efficiency. We can see that increasing the deposited mass allows improving the regeneration efficiency. Indeed, increasing the deposited mass allows increasing the cohesion forces in the cake and its resistance, which will facilitate its discharge. This observation was already reported in the literature (Sievert and Löffler, 1987; Clift and Seville, 1993) and can be used to define the maximum pressure drop value before cleaning. Increasing the number of pulses from one to 10 has a beneficial effect on the cleaning efficiency, but this is not a practical solution from an industrial point of view as it is associated with an important consumption of compressed air.

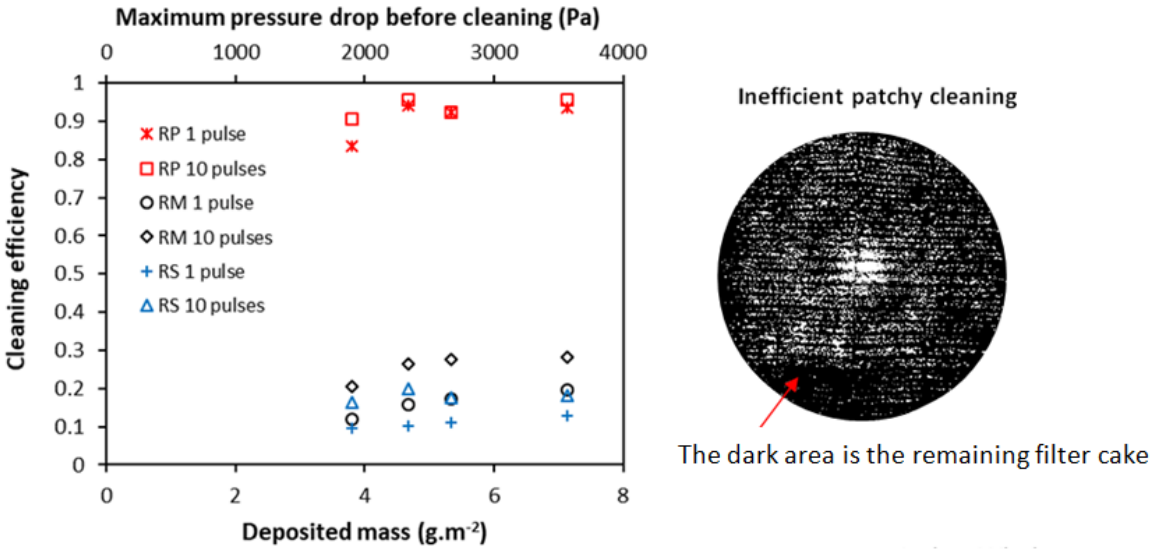

Figure 8: Cleaning efficiency of fresh filter cakes composed of metallic nanoparticles according to different parameters as a function of the deposited mass

To verify the influence of the deposited mass on the filtration process, continuous clogging/unclogging cycles were realised by fixing two values of the maximum pressure drop before cleaning. The first set at 1500 (Pa) and the second at 3000 (Pa), presented by figure 9. 10 cleaning cycles were performed using the maximum value of 1500 Pa and 20 cycles using 3000 Pa. The important evolution of the pressure drop indicates that the depth filtration phase is very brief followed by a very rapid increase due to cake formation. Similar tendencies were observed by Thomas et al. (2019) when studying the clogging of HEPA filters by graphite nanostructured particles. As shown by Li et al., (2019b) in the case of micronic particles, raising the pressure drop value before cleaning, i.e. increasing the deposited mass, improves the regeneration efficiency. Nevertheless, in both cases, the filtration process is not stable as the cycle time decreases significantly after the first cycle and the residual pressure drop value keeps increasing. This is indeed characteristic of a patchy inefficient cleaning of the filter surface. The rapid increase of the pressure drop after each cleaning corresponds to the filling of the unlogged patches. The clogging of the filters by the metallic ultrafine particles seems to be irreversible. At an industrial scale, this implies that the filters need to be replaced, raising by that operational costs.

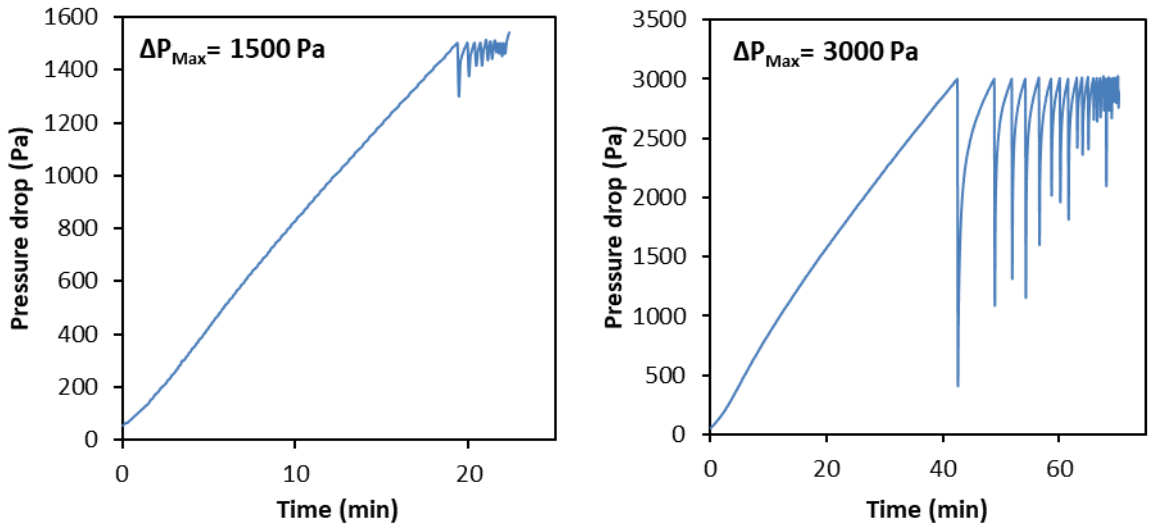

Figure 9: Influence of the maximum pressure drop value before cleaning on the filtration process.

The results of the cleaning efficiency of aged filter cakes, with a deposited mass of about 5±0.47 g.m^{-2}, stored in different conditions for 15 days are presented by figure 10. The cleaning efficiency was not evaluated according to the cleaned surface because of the cake colour change (turned to white) that made it difficult to estimate with accuracy the cleaned surface. What can be noticed is that the cleaning efficiency, according to both the residual pressure drop and the removed mass, decreases with increasing the relative humidity during storage. Exceeding a relative humidity of 60 % the cleaning efficiency reaches a minimum.

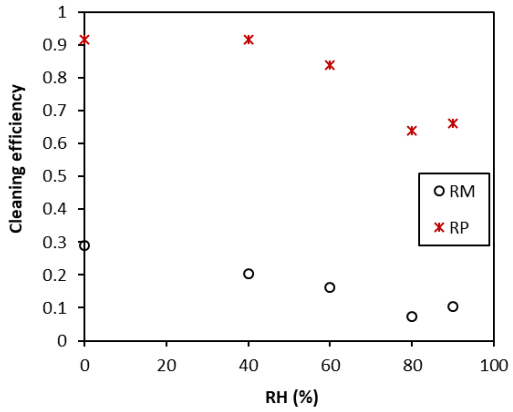

Figure 10: Variation of the cleaning efficiency of aged deposits under different humidity rates for 15 days at 15 °C.

Figure 11 gives the evolution of the adhesion force of the aged filter cakes determined by the reverse flow method. The measured adhesion force of the nanostructured deposits is of about 1000 N.m^{-2}. The order of magnitude found in the literature for filter cakes composed of micronic particles is somewhere between 50-200 N.m^{-2}. This indicates that nanostructured filter cakes are more adherent. Results show that the adhesion force increases with increasing the relative humidity. According to the previous results, the chemical nature of the filter cake has been modified which explains the variation of the adhesion force. In addition, we noted a decrease of the filter cake resistance after aging which will make its detachment more difficult. A deposit stored in dry air has the same cleaning efficiency and adhesion force as a fresh filter cake as no reaction took place (R_P= 0.95; R_M= 0.27; $F_{Adhesion}$ =1024±102 N.m^{-2}). One should note that these results give only an idea on the influence of aging on the cleaning efficiency and do not reflect a real case scenario. Indeed, the aging time and atmosphere in the industry are variable.

.

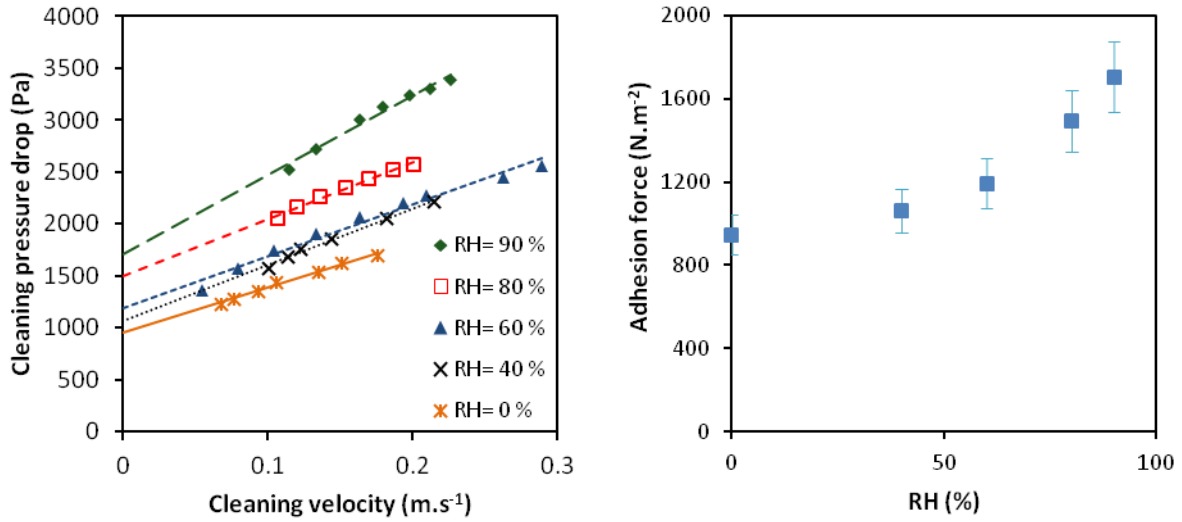

Figure 11: Variation of the adhesion force of aged deposits under different humidity rates for 15 days at 15 °C.

4. Conclusion

This study investigated the cleaning efficiency of flat filters clogged with metallic ultrafine particles using reverse pulse-jet. The influence of the deposited mass, the number of cleaning pulses and aging of the filter cake was studied. The cleaning efficiency results, evaluated according to the residual pressure drop, the removed mass and the cleaned surface, showed an inefficient patchy cleaning. Due to the formation of small holes across the filter cake, the cleaning efficiency according to the residual pressure drop reached 90% but it does not exceed 30% according to the removed mass or cleaned surface. Indeed, the unclogged patches constitute preferential passages for the airflow resulting in a decrease of the pressure drop. Hence, in the case of adhesive ultrafine dusts, the decrease of the pressure drop after cleaning does not necessarily imply that the filter surface has been fully cleaned. Moreover, increasing the maximum pressure drop before cleaning, i.e. increasing the deposited mass, allows improving the cleaning efficiency. This is associated with an increase of the cake cohesion forces and resistance that would facilitate its discharge. Clogging/unclogging cycles results showed that failing to regenerate the filter surface after each cleaning resulted in a highly unstable filtration process with a very rapid increase of the pressure drop.

The findings of this work revealed that exposing filter cakes composed of metallic nanostructured particles to different humidity conditions over time led to a decrease of the cake resistance. After aging for 22 days under 77% and 65 % relative humidity the cake resistance decreased by 87% and 60% respectively. No significant variations were registered after aging under dry air or under 30% humidity. The characterization results showed that a chemical reaction took place. Under the studied conditions, water and atmospheric CO_2 reacted with zinc leading to chemical transformation and a morphology change of the cake particles. The effect of aging for 15 days under different humidity conditions on the cleaning efficiency was also evaluated. The adhesion force between aged filter cakes and the filter showed an increase with increasing humidity during aging. This was associated with a decrease of the cleaning efficiency which went from 30% according to the removed mass after aging under dry air to 10% after aging under 80% humidity. These results confirm what was reported by the industrials and lead us to recommend avoiding leaving deposits on filter surfaces for several days or that filtration systems may have to be placed in a more controlled environment. This work gives an insight on the influence of different parameters on the cleaning efficiency that is of interest for operating industrial filtration systems.

References

Almeida, E., Morcillo, M., Rosales, B., 2000. Atmospheric corrosion of zinc Part 1: Rural and urban atmospheres. Br. Corros. J. 35, 284–288. https://doi.org/10.1179/000705900101501353

Bakri, S.F.Z., Hariri, A., Ismail, M., 2019. Metal fumes toxicity and its association with lung health problems among welders in automotive industry. J. Phys. Conf. Ser. 1150.https://doi.org/10.1088/17426596/1150/1/012001

Bémer, D., Morele, Y., Régnier, R., 2015. Filtration of ultrafine metallic particles in industry. Environ. Technol. (United Kingdom) 36, 2374–2380. https://doi.org/10.1080/09593330.2015.1028471

Bémer, D., Régnier, R., Subra, I., Sutter, B., Lecler, M.T., Morele, Y., 2010. Ultrafine particles emitted by flame and electric arc guns for thermal spraying of metals. Ann. Occup. Hyg. 54, 607–614.

https://doi.org/10.1093/annhyg/meq052

Bémer, D., Subra, I., Morele, Y., Charvet, A., Thomas, D., 2013. Experimental study of granular bed filtration of ultrafine particles emitted by a thermal spraying process. J. Aerosol Sci. 63, 25–37. https://doi.org/10.1016/j.jaerosci.2013.04.005

Charvet, A., Bau, S., Bémer, D., Thomas, D., 2015. On the importance of density in ELPI data post-treatment. Aerosol Sci. Technol. 49, 1263–1270. https://doi.org/10.1080/02786826.2015.1117568

Cho, H., Youn, J.-S., Oh, I., Jung, Y.-W., Jeon, K.-J., 2020. A new air-washing method to clean fabric filters clogged with submicron fume particles: A pilot-scale study. J. Hazard. Mater. 383, 121186. https://doi.org/10.1016/j.jhazmat.2019.121186

Clift, R., Seville, J.P.K., 1993. Gas Cleaning at High Temperatures, Springer. Springer Netherlands, Dordrecht. https://doi.org/10.1007/978-94-011-2172-9

Falcone, L.M., Erdely, A., Kodali, V., Salmen, R., Battelli, L.A., Dodd, T., McKinney, W., Stone, S., Donlin, M., Leonard, H.D., Cumpston, J.L., Cumpston, J.B., Andrews, R.N., Kashon, M.L., Antonini, J.M., Zeidler-Erdely, P.C., 2018. Inhalation of iron-abundant gas metal arc welding-mild steel fume promotes lung tumors in mice. Toxicology 409, 24–32. https://doi.org/10.1016/j.tox.2018.07.007

Falk, T., Svensson, J., Johansson, L., 1998. The role of carbon dioxide in the atmospheric corrosion of zinc. J. Electrochem. Soc. 145, 39–44.

First, M.W., Silverman, L., 1963. Predicting the performance of cleanable industrial fabric filters. J. Air Pollut. Control Assoc. 13, 581–586. https://doi.org/10.1080/00022470.1963.10468223

Gankanda, A., Cwiertny, D.M., Grassian, V.H., 2016. Role of Atmospheric CO2 and H2O Adsorption on ZnO and CuO Nanoparticle Aging: Formation of New Surface Phases and the Impact on Nanoparticle Dissolution. J. Phys. Chem. C 120, 19195–19203. https://doi.org/10.1021/acs.jpcc.6b05931

Graedel, T.E., 1989. Corrosion mechanisms for zinc exposed to the atmosphere. J. Electrochem. Soc. 136, 139–203.

Guha, N., Loomis, D., Guyton, K.Z., Grosse, Y., El Ghissassi, F., Bouvard, V., Benbrahim-Tallaa, L., Vilahur, N., Muller, K., Straif, K., 2017. Carcinogenicity of welding, molybdenum trioxide, and indium tin oxide. Lancet Oncol. 581–582. https://doi.org/10.1016/S1470-2045(17)30255-3

Hau, C.W.Y., Leung, W.W.F., 2016. Experimental investigation of backpulse and backblow cleaning of nanofiber filter loaded with nano-aerosols. Sep. Purif. Technol. 163, 30–38. https://doi.org/10.1016/j.seppur.2016.02.041

Joubert, A., Laborde, J.C., Bouilloux, L., Callé-Chazelet, S., Thomas, D., 2010. Influence of humidity on clogging of flat and pleated HEPA filters. Aerosol Sci. Technol. 44, 1065–1076.
https://doi.org/10.1080/02786826.2010.510154

Li, S., Hu, S., Xie, B., Jin, H., Xin, J., Wang, F., Zhou, F., 2019a. Influence of pleat geometry on the filtration and cleaning characteristics of filter media. Sep. Purif. Technol. 210, 38–47. https://doi.org/10.1016/j.seppur.2018.05.002

Li, S., Wang, F., Xin, J., Xie, B., Hu, S., Jin, H., Zhou, F., 2019b. Study on effects of particle size and maximum pressure drop on the filtration and pulse-jet cleaning performance of pleated cartridge filter. Process Saf. Environ. Prot. 123, 99–104. https://doi.org/10.1016/j.psep.2019.01.002

Michalek, I.M., Martinsen, J.I., Weiderpass, E., Hansen, J., Sparen, P., Tryggvadottir, L., Pukkala, E., 2019. Heavy metals, welding fumes, and other occupational exposures, and the risk of kidney cancer: A population-based nested case-control study in three Nordic countries. Environ. Res. 173, 117–123. https://doi.org/10.1016/j.envres.2019.03.023

Montgomery, J.F., Green, S.I., Rogak, S.N., 2015. Impact of relative humidity on HVAC filters loaded with hygroscopic and non-hygroscopic particles. Aerosol Sci. Technol. 49, 322–331. https://doi.org/10.1080/02786826.2015.1026433

Schmidt, E., Pilz, T., 1996. Raw gas conditioning and other additional techniques for improving surface filter performance. Filtr. Sep. 33, 409–415. https://doi.org/10.1016/S0015-1882(97)84301-7

Seville, J.P.K., Cheung, W., Clift, R., 1989. A patchy-cleaning interpretation of dust cake release from non-woven fabrics. Filtr. Sep. May/June, 187–190.

Sievert, J., Löffler, F., 1987. Dust cake release from non woven fabrics. Filtr. Sep. 424–427.

Silva, C.R.N., Negrini, V.S., Aguiar, M.L., Coury, J.R., 1999. Influence of gas velocity on cake formation and detachment. Powder Technol. 101, 165–172. https://doi.org/10.1016/S0032-5910(98)00168-5

Tanabe, E.H., Barros, P.M., Rodrigues, K.B., Aguiar, M.L., 2011. Experimental investigation of deposition and removal of particles during gas filtration with various fabric filters. Sep. Purif. Technol. 80, 187–195. https://doi.org/10.1016/j.seppur.2011.04.031

Thomas, D., Pacault, S., Charvet, A., Bardin-Monnier, N., Appert-Collin, J.C., 2019. Composite fibrous filters for nano-aerosol filtration: Pressure drop and efficiency model. Sep. Purif. Technol. 215, 557–564. https://doi.org/10.1016/j.seppur.2019.01.043

Xie, B., Li, S., Chu, W., Liu, C., Hu, S., Jin, H., Zhou, F., 2020. Improving filtration and pulse-jet cleaning performance of metal web filter media by coating with polytetrafluoroethylene microporous membrane. Process Saf. Environ. Prot. 136, 105–114. https://doi.org/10.1016/j.psep.2020.01.002

Young, J.F., 1967. Humidity control in the laboratory using salt solutions-a review. J. Appl. Chem. 17, 241–245. https://doi.org/10.1002/jctb.5010170901